International Journal of Inventive Engineering and Sciences (IJIES)
ISSN: 2319-9598 (Online), Volume-10 Issue-9, September 2023

Crosstalk Characterization and Reduction in Power Lines

Jacquie Therese NGO BISSE, Bedel Giscard ONANA ESSAMA, Joseph KOKO KOKO, Jacques ATANGANA, Salomé NDJAKOMO ESSIANE

Abstract: ***We propose a technique of crosstalk reduction through power lines. This crosstalk reduction technique utilises the pseudo-matched impedances method, which determines the characteristic parameters of the chosen line using transmission line theory. Besides, we establish the telegrapher's equations to determine the characteristic impedances of the line. Further, two types of lines are employed here to apply the pseudo-matched impedances method. The far- and near-end crosstalk is measured using two strategies: a Simulink diagram and a MATLAB code. The Simulink diagram of the power line provides crosstalk curves, and the Matlab code directly returns crosstalk values. The crosstalk reduction rate appears to be between 20% and 50%, compared to previous investigations using pseudo-matched impedances in the literature. Moreover, the variation of two different types of impedances leads to a crosstalk reduction rate that approaches 99%.***

Keywords: ***Crosstalk, Far-End Crosstalk, Near-End Crosstalk, Pseudo Adapted Impedances, Electromagnetic Compatibility.***

I. INTRODUCTION

The source can represent any device or physical-electrical phenomenon that induces electromagnetic disturbances by conduction or radiation. Among the leading causes of disorders, we can name the distribution of electrical energy, the propagation of radio waves, electrostatic discharges, electric motors, lightning, and other related phenomena.

The crosstalk phenomenon stands for the interference induced by the electromagnetic waves that influence the electric signals sent through power network lines [1-5].

Manuscript received on 29 July 2023 | Revised Manuscript received on 09 September 2023 | Manuscript Accepted on 15 September 2023 | Manuscript published on 30 September 2023.
*Correspondence Author(s)
Dr. Jacquie Therese NGO BISSE[1], Email: jacquieday13@gmail.com
Dr. Bedel Giscard ONANA ESSAMA[2]*, Email: onanaessama@yahoo.fr, ORCID ID: 0000-0002-9900-0419
Dr. Joseph KOKO KOKO[3], Email: kokojoseph469@yahoo.fr
Prof. Jacques ATANGANA[4], Email: acquesatangana215@yahoo.com
Prof. Salomé NDJAKOMO ESSIANE[5], Email: salomendjakomo@gmail.com
(1,2,3,5) Laboratory of Electrotechnics, Automatics and Energy, Department of Electrical Engineering, Higher Technical Teachers ' Training College (HTTTC) of Ebolowa, University of Ebolowa, P.O. Box 886 Ebolowa, Cameroon
(1,2,5) Cameroonian Association for Research and Innovation in Environmental and Energetic Technologies (ACRITEE), P.O. Box 59 Ebolowa, Cameroon
(4) Higher Teacher Training College of Yaounde, University of Yaounde I, P.O. Box 47, Yaounde, Cameroon.

Moreover, the crossalk phenomenon also acts in optical transmission network cables. In this case, this phenomenon affects data communication in data centres, server rooms, and other areas where a constant flow of data is necessary. The crosstalk phenomenon is a common issue that is addressed to facilitate improved networking and data transfer. Furthermore, there are two types of crosstalk phenomena which affect networks in various ways. Those crosstalk types are named near-end crosstalk and far-end crosstalk [1-5]. All the types of crosstalk are generated inductively (parasitic mutual inductance) or capacitively (parasitic mutual capacitance). Inductive crosstalk is only generated when the aggressor signal modifies the levels. Hence, higher speed signals generate stronger crosstalk. Besides, the capacitive crosstalk is generated by changing the potential difference between the two interconnects [1-5]. In circuit models describing interconnects, mutual inductance and capacitance are used to describe the coupling between the aggressor and victim drivers [1-5].

There are several techniques to prevent and reduce the electromagnetic perturbations (crosstalk) so that they do not affect victim drivers. Among the victim drivers, we note two cases. The first one concerns the powered driver that receives an external disturbance. Additionally, the second case involves a non-powered driver who gets an external disturbance. The investigation of this paper focuses on the last case [1-5].

Moreover, we precisely study the case of two drivers where the powered driver affects the non-powered one. This case is frequently observed in the interconnections of power transmission lines. Furthermore, one question arises: what can be done to mitigate or delay this phenomenon? It is well known that to fight against those electromagnetic phenomena or radiation coupling, we can minimize ground loops, use shielding and/or move the victim receiver away from the source of disturbances [1-5]. Those techniques cannot provide a better solution to address the crosstalk problem caused by near-field coupling in interconnected lines. Moreover, crosstalk phenomena have also been on other physical systems such as light wave networks [6-12], bus networks [13], and gene networks [14-19]. However, the use of the pseudo-matched impedances method to reduce and characterise crosstalk phenomena in power lines has been reported least in the literature. The paper is organized as follows. In Section 2, we establish the equations of the telegrapher's line to determine the characteristic parameters of the studied line. Then, we develop the pseudo-matched impedances method and characterise the crosstalk phenomenon.

In Sec. 3, we present the results and discussion of numerical simulations corresponding to the crosstalk reduction on the line under consideration. Thereafter, the outcomes are compared to some results previously obtained in literature. In Sec.4, we summarize.

II. MATHEMATICAL DEVELOPMENT AND THE MODEL

We utilise the computer and MATLAB software as key tools to solve the crosstalk problem. The investigation includes both analytical and numerical aspects. The analytical element involves determining characteristic parameters related to the electric power transmission line. From those parameters, we establish the mathematical models, including the voltage, current, and characteristic impedance matrices of the line. Those different matrices associated with pseudo-adapted impedances are inserted at the ends of the lines. Furthermore, the numerical aspect of this method involves simulating a two-driver line model with pseudo-matched impedances. Those simulations will be done in the MATLAB 2018a environment.

A. Transmission Line Theory

We consider the diagram of Fig. (1) illustrating a model of transmission line [20].

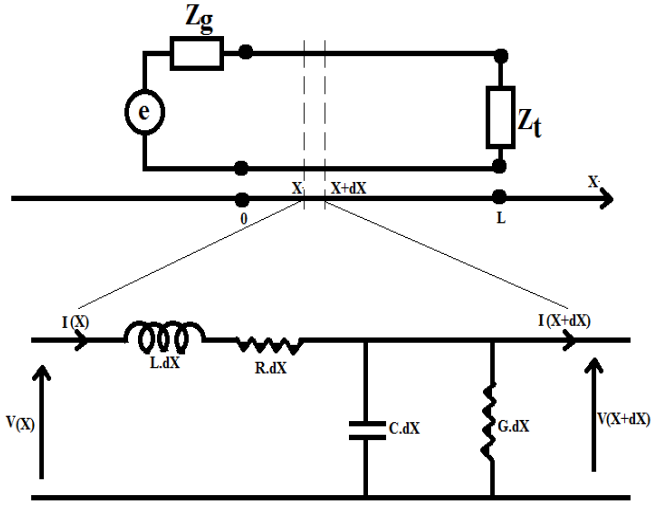

Figure 1 – Model of Transmission Line Considered [20].

Considering the characteristic parameters of the circuit (R, L, C and G), and the second derivative, the telegraphers' equations are obtained as follows [20]:

$$-\frac{\partial^2 V}{\partial x^2} = LC.\frac{\partial^2 V}{\partial t^2} + (RC + LG).\frac{\partial V}{\partial t} + RG.V \quad (1)$$

$$-\frac{\partial^2 I}{\partial x^2} = LC.\frac{\partial^2 I}{\partial t^2} + (RC + LG).\frac{\partial I}{\partial t} + RG.I. \quad (2)$$

In the sinusoidal regime and introducing the complex form, the telegraphers' equations become [20]:

$$-\frac{d^2 V}{dx^2} = ZY.V(x) \quad (3)$$

$$-\frac{d^2 I}{dx^2} = ZY.I(x) \quad (4)$$

with $Z = R + j\omega L$ and $Y = G + jC\omega$.

B. Pseudo-Matched Impedances' Method

This method involves introducing impedances at the ends of the line to cancel reflections when the pseudo-matched impedances are equivalent to the line's characteristic impedance.

a. Characteristic Impedance of the Line

The matching network of a two-drivers line has the role of absorbing the waves coming from the end where it is connected and not generating reflected waves.

To cancel the reflections occurring at the ends of the lines, a termination with an impedance matrix equal to the characteristic impedance matrix [Zc] of the CML is connected at each end of the line (see Fig. (2)).

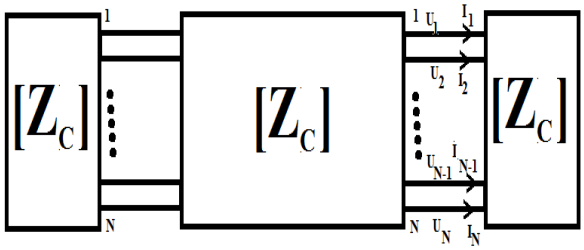

Figure 2. Illustration of MCL with Characteristic Impedance at the Ends [21].

Let us consider the case of a line with two drivers. The following characteristic impedance matrix characterizes this line]:

$$[Zc] = \begin{bmatrix} Z_{C11} & Z_{C12} \\ Z_{C12} & Z_{C11} \end{bmatrix} \quad (5)$$

According to the definition of the matrix [Zc], the following equation can be verified [21]:

$$[U]=[Zc].[I] \quad (6)$$

where $[U] = \begin{bmatrix} U_1 \\ U_2 \end{bmatrix}$ et $[I] = \begin{bmatrix} I_1 \\ I_2 \end{bmatrix}$.

Combining Eqs. (7) and (8) yield Eqs. (9) and (10) as follows [21]:

$$U_1 = Z_{C11}.I_1 + Z_{C12}.I_2 \quad (7)$$

$$U_2 = Z_{C12}.I_1 + Z_{C11}.I_2. \quad (8)$$

We can therefore deduce the admittance expression as follows[21]:

$$Y_0 = [Zc]^{-1}. \quad (9)$$

The matrices [Z] and [Y] are frequency-dependent and defined from the matrices of the linear parameters of the line. In addition, we neglect R and G. So, we obtain [21]:

$$[ZjL] \quad (10)$$

$$[Y] = j \cdot \omega \cdot [C] \quad (11)$$

Equations (10) and (11) are obtained in the case of a lossless line.

Retrieval Number: 100.1/ijies.C78830912323
DOI: 10.35940/ijies.C7883.0910923
Journal Website: www.ijies.org

Published By:
Blue Eyes Intelligence Engineering and Sciences Publication (BEIESP)

b. Modelling of Crosstalk Phenomenon

The illustration of the crosstalk phenomenon is done by considering three drivers, impedances, and a power source as depicted in Fig. 3. We investigate the case of a lossless line. The quantities V_{NE} (t) and V_{FE} (t) are induced voltages coming from the currents induced in the circuit. The term V_{NE} (t) corresponds to the near-end crosstalk and V_{FE} (t) stands for the far-end crosstalk. Thereafter, the pseudo-matched impedances are determined and are represented as follows:

$Z_c = R_s$; $Z_c = R_{NE}$; $Z_c = R_{NF}$; $Z_c = R_L$

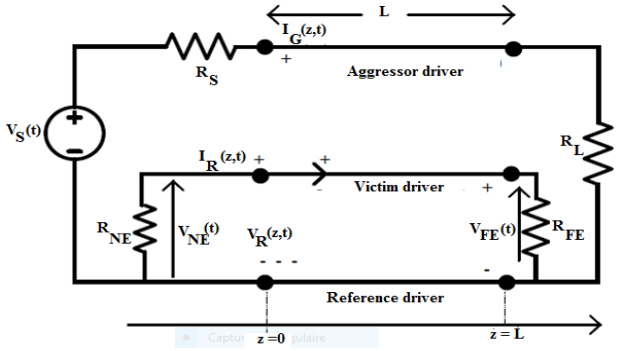

Figure 3 - Unshielded Line Composed of three Drivers [21, 22].

c. Initial conditions at the beginning of the simulation

Those conditions are presented in Table 1 as follows.

Table 1 - The Values of the Line Parameters

Lines		
Linear inductance (µH/m)	$L1=\begin{bmatrix}0.8629 & 0.3725\\ 0.3725 & 0.8629\end{bmatrix}$	$L2=\begin{bmatrix}0.9337 & 4.1264\\ 4.1264 & 0.9337\end{bmatrix}$
Linear capacity (pF/m)	$C1=\begin{bmatrix}46.762 & -18.036\\ -18.036 & 46.762\end{bmatrix}$	$C2=\begin{bmatrix}12.74 & 7.751\\ 7.751 & 12.74\end{bmatrix}$
Impedance (ohm)	$Z_{C1}=\begin{bmatrix}147.1874 & 60.1923\\ 60.1923 & 147.1874\end{bmatrix}$	Zc2=444.1967
Length (km)	d=100	
Number of drivers	N=2	
Sources		
Voltage(V)	U=250000	
Frequency (Hz)	f=50	
Phase shift (degree)	$\varphi = 15°; 30°; 60°; 90°$	

d. Matlab Code

```
f=50;     (Frequency)
U=250000;   (voltage)
d=10000;      (length of propagation)
n=2;          (number of drivers)
l=[0.8629 0.3725; 0.3725 0.8629] ;  (Linear inductance)
c=[46.762 -18.036; -18.036 46.762] ; (Linear capacity)
L=l*d;
C=c*d;
w=2*pi*f;          (Angular frequency)
Zc=(L/C)^(1/2);   (characteristic impedance of the line)
Y=w*C;             (line admittance )
Z=w*L;             (line impedance)
γ = √(Z.Y)         (Propagation coefficient)
Z1= Z2= Z3= Z4=Zc;
```

e. Schematic Diagram

The schematic diagram is illustrated in Fig.(4) in Appendix. This Fig.(4) presents a multi-drivers line (middle block) which is supplied with voltage from the first block on the left. The middle block consists of three drivers, pseudo-matched impedances, and current and voltage measurement devices. The last block on the right is used to observe the curves (see Fig.(4) in Appendix).

C. The Model

a. Electrical Diagram

The crosstalk phenomenon can be implemented in the MATLAB environment by the diagram depicted in Fig.(5).

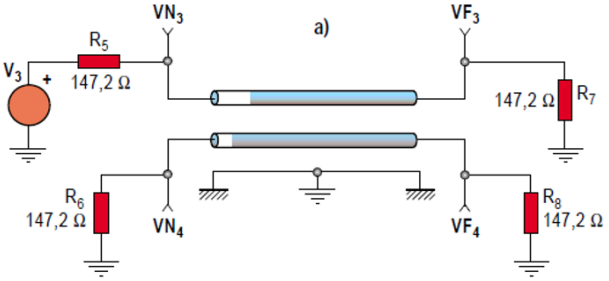

Figure 5- Network Configuration [23].

III. RESULTS AND DISCUSSION

A. Simulations using Matlab Code

The linear parameters provided in the mathematical development in Sec. 2 are inserted into the MATLAB code. A sinusoidal signal is injected on the line at the beginning of propagation. Therefore, the disturbed line obtained here can allow the evaluation of the far-end and near-end crosstalk voltages on the second line (or victim driver).

a. Results of Matlab Code

We utilise the line parameters presented in Table 1 to implement the MATLAB code shown in Section 2.2.4. The results are then listed in Table 2.

Table 2- Results Obtained with Two Types of Lines

Z_C= 147.1874 ohms			
Near-End crosstalk	Far-End crosstalk	Phase shift (°)	Reduction rate
8.09kV	0V	30	**100%**
24.92kv	0V	60	
29KV	0V	90	
Zc=444.1967 ohms			
Near-End - crosstalk	Far-End - crosstalk	Phase shift (°)	Reduction rate
15.182KV	0V	30	**100%**
26.296kv	0V	60	
30.364KV	0V	90	

We have here an overview of the results of near-end crosstalk and Far-end crosstalk in this table

B. Configuration of the Power Line

a. Configuration of the First Power Line for the Zc1 Impedance

Initially, we use the setup in Fig. 5 to characterise the crosstalk with the pseudo-matched impedances of 147.2 Ω. Thereafter, we can observe the manifestation of crosstalk.

Additionally, the far-end and near-end crosstalk will be measured at points VN4 and VF4, respectively. Besides, another measurement can be directly done through Fig. (6) illustrated in Appendix.

b. Configuration of the Second Line with Zc2 Impedance

The value of the impedance changes to Zc2 = 444.196 Ω, and we inject a new signal on the line. In the second configuration, the new impedance will enable us to verify whether our method effectively reduces or delays the crosstalk phenomenon on the line. Each impedance must be connected to the end of the line under consideration.

c. Study Principle

The studied structure is supplied with a voltage source using constant amplitude and frequency. Then, we measure the induced voltage on the neighbouring line (victim driver). The measurement of the crosstalk is done at the V_{NE} point (see Fig. (3)), using the scope when the line is powered by a voltage of 250Kv. The same source is applied in simulation using MATLAB at a frequency of 50 Hz.

C. Impact of Phase Shift on the Crosstalk Phenomenon

a. Crosstalk Phenomenon on a Line with Zc=147.1874 ohms and φ=15°.

We obtain Fig. (7) for Zc=147.1874 ohms and φ=15°. The voltage injected in the line is depicted in Fig. 7(a). The injected voltage has a sinusoidal form with a period of T = 0.02 s. The amplitude of this injected curve is 1.25×10^5 v as depicted in Fig. 7(a). Additionally, the introduction of near-end crosstalk reduces the voltage amplitude from 1.25 × 10^5 V to 2.50 × 10^4 V, as illustrated in Figure. 7(a) and (b). The beginning of the propagation is shifted from 0 V to 1.00 × 10^4 V, as seen in Figs. 7(a) and (b). Further, a fluctuation corresponding to a broken point appears at the beginning of the propagation at $T=0.6\times10^{-3}$ s as depicted in Fig. 7(b). Moreover, the fluctuation exhibits a horizontal and constant behaviour when 0 < T < 0.6 × 10^(-3) s. This behaviour becomes vertical and constant at T = 0.6 × 10^ (-3) s, when the amplitude varies between 0.6 × 10^4 V and 1.0 × 10^4 V, as depicted in Fig. 7(b). Thereafter, the behaviour of the voltage changes from a vertical and constant form to a sinusoidal form for T > 0.6 × 10^ (- 3) s, as depicted in Fig. 7(b). It appears that the behaviour exhibited in Fig. 7(b) corresponds to the main behaviour of the near crosstalk when Zc=147.1874 ohms and φ=15°. The near-end crosstalk value is 1.0 × 10^4 V = 10 kV, as depicted in Fig. 7(b).

The introduction of far-end crosstalk alters the nature of the broken point, as shown in Fig. 7(c). Additionally, the voltage curve exhibits an ascending and linear behaviour when 0 < T < 0.6 × 10^(-3) s. This behaviour changes from ascendant and linear to vertical and constant when T = 0.6 × 10^ (-3) s, as illustrated in Fig. 7(c). Moreover, the vertical and continuous behaviour of the voltage varies between 0 V and 520 V, as depicted in Fig. 7(c). Furthermore, the voltage behaviour changes again from vertical and constant to horizontal and constant when T > 0.6 × 10^(-3) s, as shown in Fig. 7(c). It appears that the strange behavior described in Fig 7(c) constitutes the main behavior of the far-end crosstalk when Zc=147.1874 ohms and φ=15°. The far-end crosstalk value is 520 V, equivalent to 0.52 kV, as depicted in Fig. 7(c).

b. Crosstalk Phenomenon with Zc=147.1874 ohms and φ=30°.

The impedance is maintained at Zc = 147.1874 ohms, and the phase shift increases from φ = 15 ° to φ = 30 °. The growth of the phase shift modifies the form of the injected curve from a sinusoidal form to a linear form, as depicted in Figs. 7(a) and 8(a). Additionally, the linear and ascending behaviour of the voltage curve exhibits a breakpoint at T = 0.6 × 10^ (-3) s. Furthermore, this linear form varies between -0.2 × 10^4 V and 3.8 × 10^4 V, as depicted in Fig. 8(a).

The introduction of near-end crosstalk leads to Fig. 8(b). The sinusoidal voltage associated with a slight fluctuation, as seen in Fig. 7(b), is transformed into the large, broken structure depicted in Fig. 8(b). The previously small, broken point in the linear source voltage, as shown in Fig. 8(a), has significantly increased, as observed in Fig. 8(b). The near-end crosstalk curve progressively increases (ascendant behavior) from 9500 v to 9800 v when $0<T<0.6\times10^{-3}$ s as illustrated in Fig. 8(b). Thereafter, we observe a vertical and constant decrease from 9800 V to 5000 V when T = 0.6 × 10^ (-3) s. Then, the curve undergoes a steep and linear increase (ascendant behaviour) from 5000 V to 8000 V when T > 0.6 × 10^ (- 3) s, as depicted in Fig. 8(b).

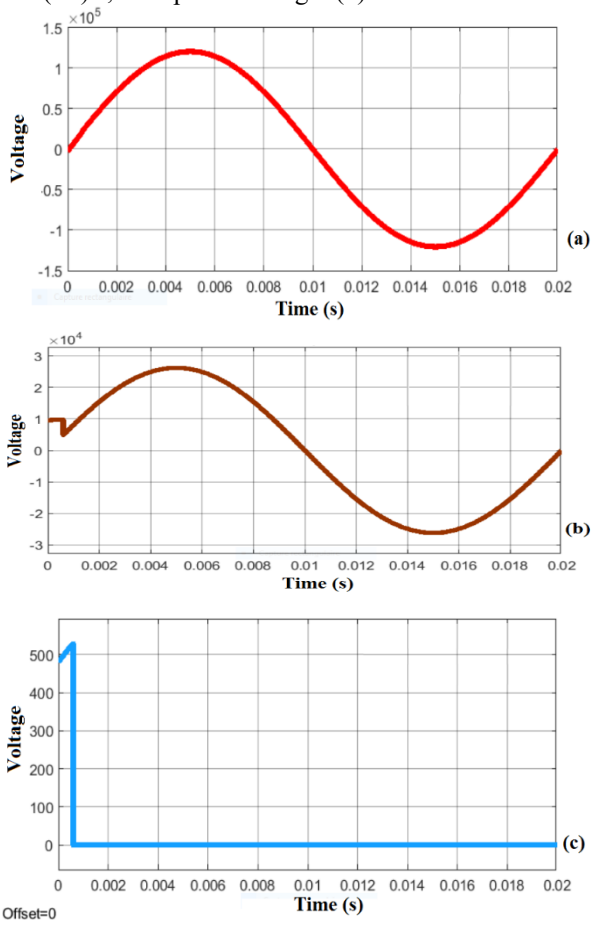

Figure 7: Crosstalk Curves for z=147.182 ohms and φ=15°: (a) Source Voltage; (b) Near-End Crosstalk; (c) Far-end Crosstalk.

Retrieval Number: 100.1/ijies.C78830912323
DOI: 10.35940/ijies.C7883.0910923
Journal Website: www.ijies.org

Published By:
Blue Eyes Intelligence Engineering and Sciences Publication (BEIESP)

The introduction of the far-end crosstalk leads to Fig. 8(c), where the massive broken structure still appears. However, the voltage values have significantly decreased. The far-end crosstalk curve gradually increases (ascendant behavior) from 4900 v to 5300 v when $0<T<0.6\times10^{-3}$ s as depicted in Fig. 8(c). Thereafter, we observe a vertical and constant decrease (in linear form) from 5300 V to 0 V when T = 0.6 × 10^ (-3) s. Besides, the curve exhibits a constant and horizontal behaviour (linear form) close to 0 V when T > 0.6 × 10^ (- 3) s, as presented in Fig. 8(c).

It appears that the near-and far-ends crosstalk exhibit the same behaviors (Huge broken structure) when the phase shift is fixed to φ=30°. However, the voltage values associated with each effect differ, as shown in Figs. 8 (b) and (c). Consequently, the introduction of the crosstalk phenomenon significantly decreases the voltage values.

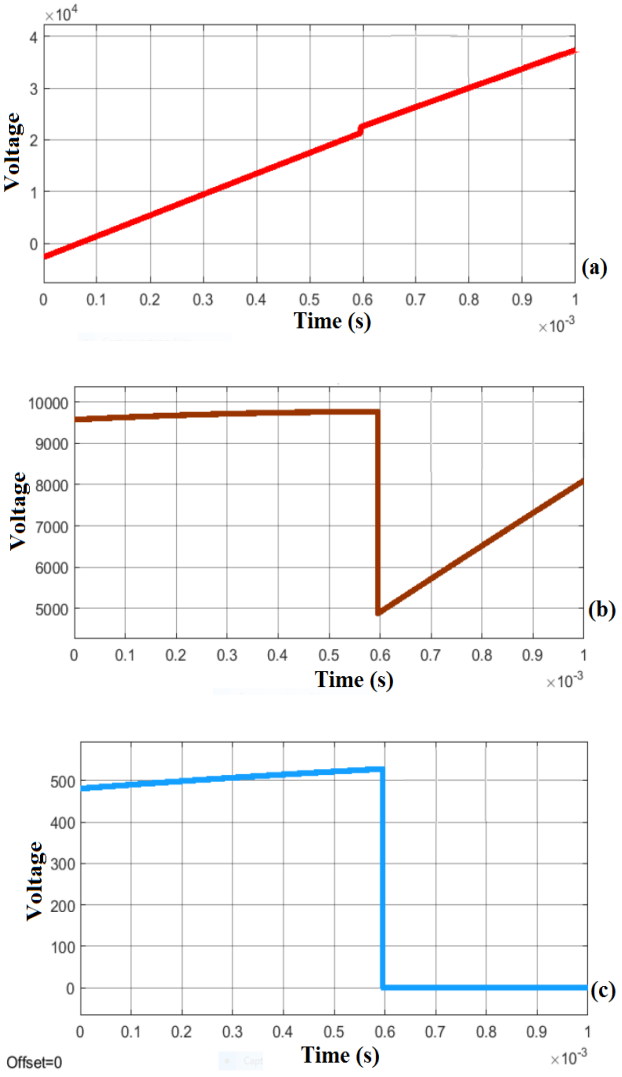

Figure 8- Crosstalk Curves for z=147.182 ohms and φ=30°: (a) Source Voltage, (b) Near-End Crosstalk, (c) Far-End Crosstalk.

It appears that the increase in phase shift significantly modifies the impact of the crosstalk phenomenon on the source voltage, as illustrated in Figs. (7) and (8).

c. Crosstalk Phenomenon with Zc=147.1874 ohms and φ=60°.

The impedance is maintained at Zc = 147.1874 ohms, and the phase shift is increased from φ = 30 ° to φ = 60 °. Then, we obtain Fig. (9). The source voltage has changed its aspect from the precedent linear form depicted in Fig. 8(a) to the sinusoidal form illustrated in Fig. 9(a). This sinusoidal curve exhibits a slight fluctuation at the beginning of wave propagation at T = 0.5 × 10^ (-3) s, as shown in Fig. 9(a).

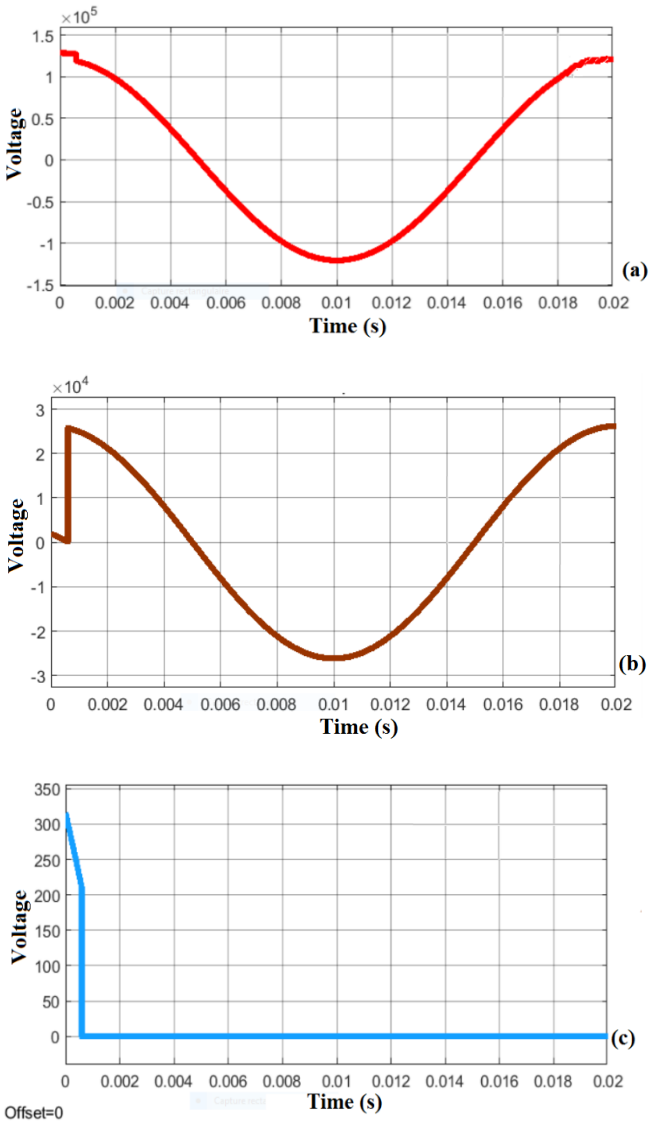

Figure 9- Crosstalk Curves for z=147.182 ohms and φ=60°: (a) Source Voltage; (b) Near-End Crosstalk; (c) Far-End Crosstalk.

The introduction of near-end crosstalk creates a significant discontinuity at the beginning of propagation, as shown in Fig. 9(b). The near-end crosstalk curve exhibits a slight linear decrease (descendant behaviour) from 0.2×10^4 V to 0 V when $0 < T < 0.5 \times 10^{(-3)}$ s. Then, the curve exhibits a steep vertical and constant increase from 0 V to 2.7 × 10^4 V when T = 0.5 × 10^ (-3) s, as illustrated in Fig. 9(b). More so, the curve maintains its sinusoidal aspect when $T=0.5\times10^{-3}$s as illustrated in Fig. 9(b).

The introduction of far-end crosstalk distorted the sinusoidal form into a strange, broken form, as depicted in Figs. 9 (b) and (c). The new form exhibits many steps. The curve exhibits a linear decrease from 320 V to 210 V when 0 < T < 0.5 × 10^ (- 3) s, as shown in Fig. 9(c). Additionally, the curve exhibits a vertical and constant behaviour from 210 V to 0 V when T = 0.5 × 10^ (-3) s. Furthermore, the curve exhibits a continuous and horizontal behaviour close to 0 V when T > 0.5 × 10^ (- 3) s, as shown in Fig. 9(c).

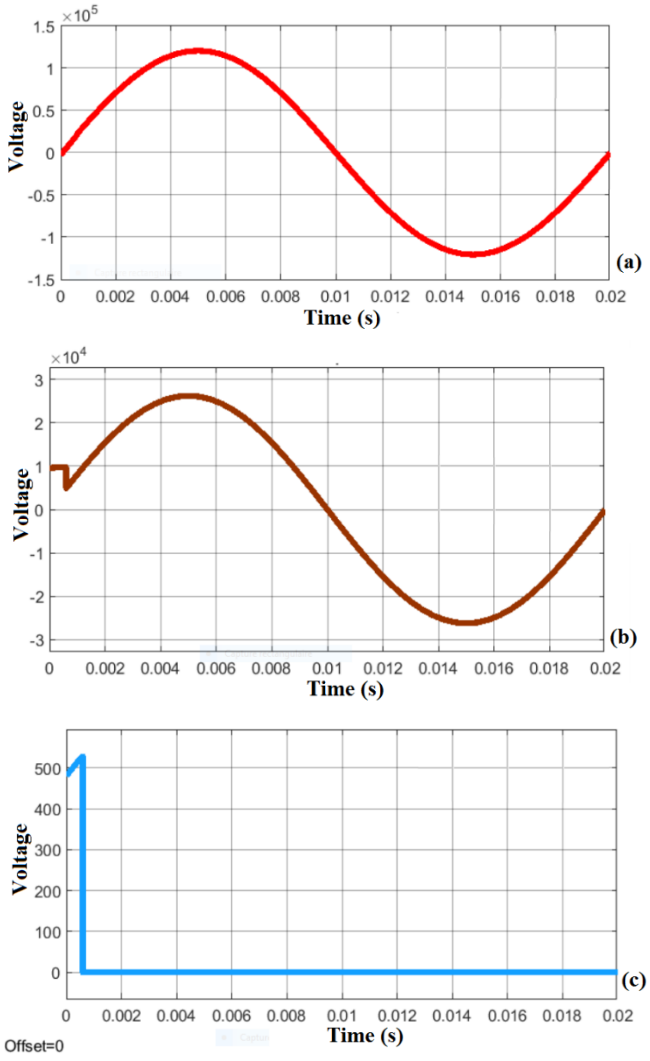

Figure 10- Crosstalk Curves for z=147.182 ohms and φ=90°: (a) Source Voltage; (b) Near-End Crosstalk; (c) Far-End Crosstalk.

d. Crosstalk Phenomenon with Zc=147.1874 ohms and φ=90°.

The impedance is maintained at Zc = 147.1874 ohms, and the phase shift increases from φ = 60 ° to φ = 90 °. Then, Fig. (10) is obtained. The source voltage maintains its sinusoidal form, characterised by an amplitude of approximately 1.25 × 10 ^5 V, as depicted in Fig. 10(a). However, the introduction of the near-end crosstalk induces a decrease of amplitude from 1.25×10^5 v to 2.70×10^4 v as illustrated in Figs—10 (a) and (b). Moreover, a slight fluctuation is also observed at the beginning of propagation, as seen in Fig. 10(b). Besides, the near-end crosstalk curve undergoes a constant and horizontal behavior (linear form) with an amplitude of 1.00×10^4 v when $0<T<0.5\times10^{-3}$ s as depicted in Fig. 10(b). Thereafter, the curve exhibits a vertical and constant behaviour, leading to a decrease in voltage from 1.00 × 10^4 V to 0.50 × 10^4 V when T = 0.5 × 10^-3 s, as depicted in Fig. 10(b). Furthermore, the sinusoidal form is maintained when T > 0.5 × 10^ (- 3) s, as seen in Fig. 10(b).

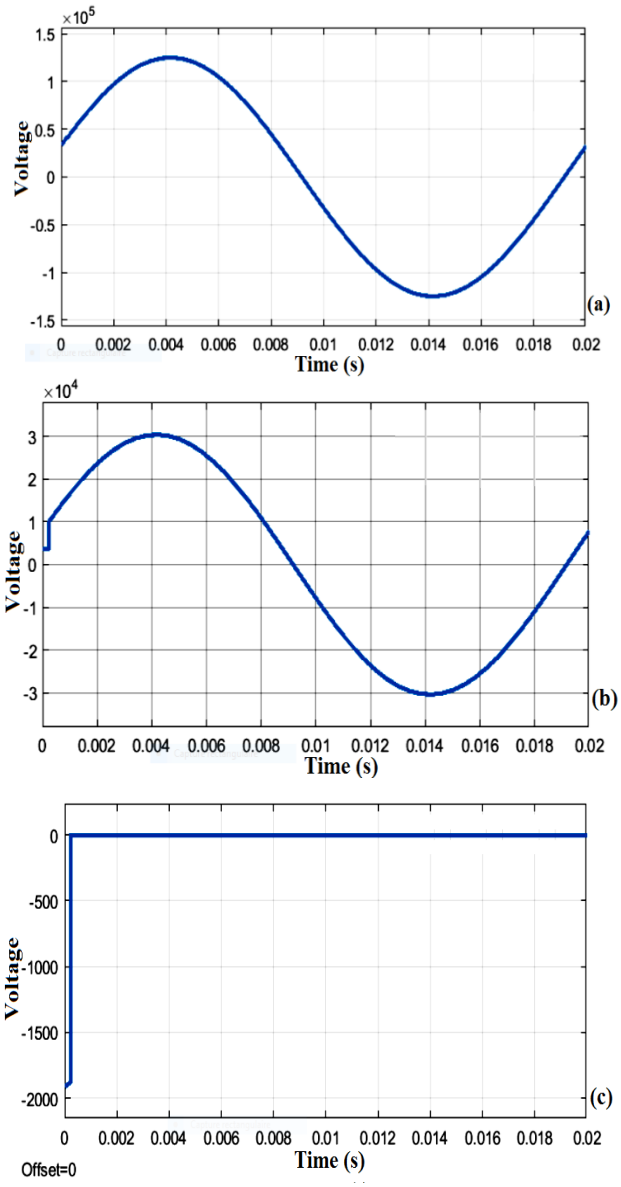

Figure 11 - Crosstalk Curves for z=444.196 ohms and φ=15°: (a) Source Voltage; (b) Near-End Crosstalk; (c) Far-End Crosstalk.

The introduction of the far-end crosstalk modifies the nature of the broken point as seen in Fig. 10(c). Additionally, the voltage curve exhibits an ascending and linear behaviour from 500 V to 520 V when 0 < T < 0.5 × 10^(-3) s. This behaviour changes from ascendant and linear to vertical and constant at T = 0.5 × 10^ (-3) s, as illustrated in Fig. 10(c). Moreover, the vertical and continuous behaviour of the voltage decreases from 520 V to 0 V, as depicted in Fig. 10(c). Furthermore, the voltage behaviour changes again from vertical and constant to horizontal and constant when T > 0.5 × 10^(-3) s, as shown in Fig. 10(c). It appears that the crosstalk phenomenon modifies the system in the same way for two different values of phase shift (φ = 15 ° and φ = 90 °), as depicted in Figs. (7) and (10).

Retrieval Number: 100.1/ijies.C78830912323
DOI: 10.35940/ijies.C7883.0910923
Journal Website: www.ijies.org

Published By:
Blue Eyes Intelligence Engineering and Sciences Publication (BEIESP)

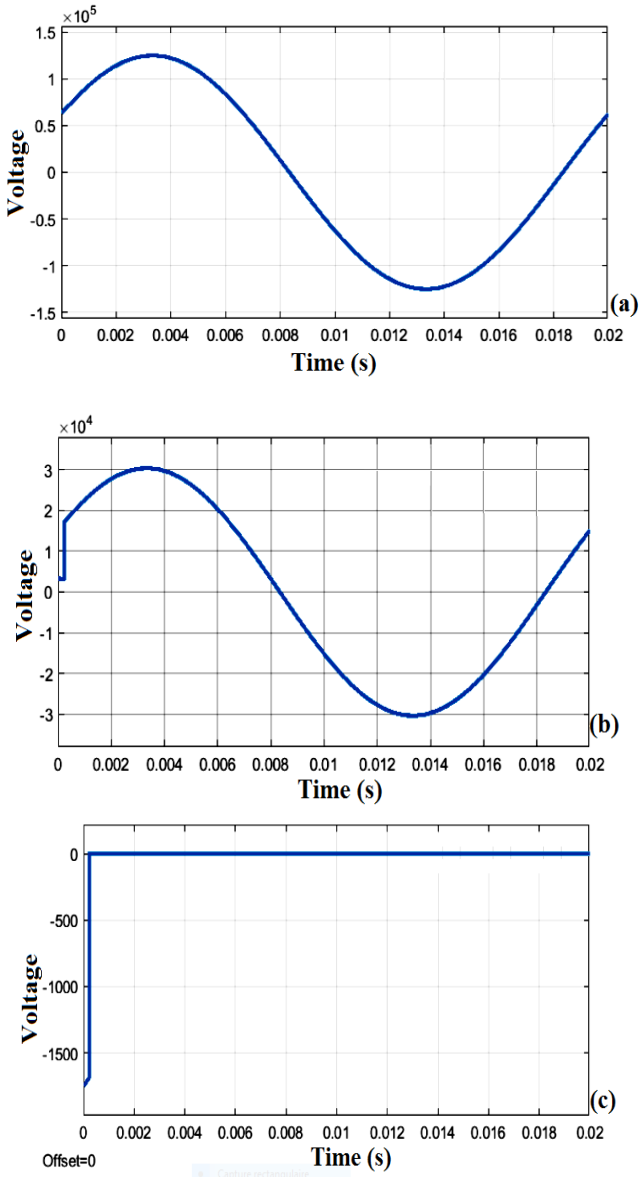

Figure 12 - Crosstalk Curves for z=444.196 ohms and φ=30°: (a) Source Voltage; (b) Near-End Crosstalk; (c) Far-End Crosstalk.

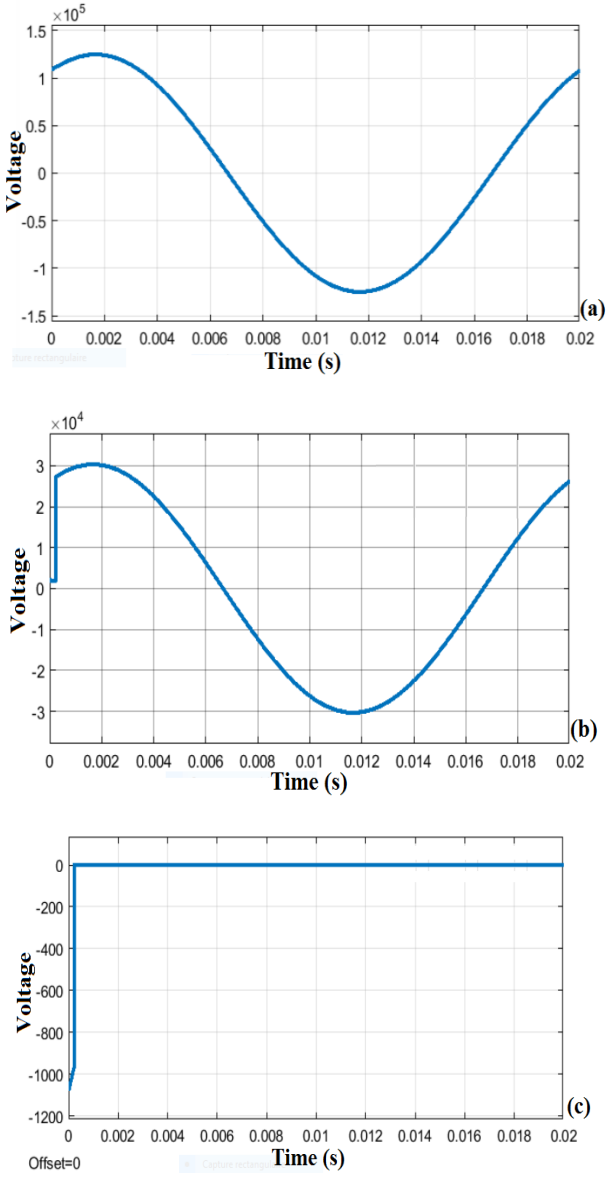

Figure 13 - Crosstalk Curves for z=444.196 ohms and φ=60° : (a) Source Voltage; (b) Near-End Crosstalk; (c) Far-End Crosstalk.

D. Impact of the Impedance on the Crosstalk Phenomenon

a. Crosstalk Phenomenon with Zc=444.196 ohms and φ=15°.

The phase shift is maintained at φ = 15 °, and the impedance is modified from Zc = 147.1874 ohms to Zc = 444.196 ohms. We obtain Fig. (11). Compared to Fig. (7), the source voltage begins the propagation at 0.5×10^5 v as seen in Fig. 11(a). The introduction of the near-end crosstalk induces a small fluctuation at the beginning of the propagation. Besides, the time of apparition of this fluctuation has decreased from 0.5×10^{-3} s to 0.1×10^{-3} s as depicted in Figs. 7(b) and 11(b). Furthermore, the curve exhibits a linear and constant behaviour at 0.3 × 10^4 V when 0 < T < 0.1 × 10^(-3) s, as shown in Fig. 11(b). The curve undergoes a small vertical and constant behavior from 0.3×10^4 v to 1.00×10^4 v when $T=0.1\times10^{-3}$ s as illustrated in Fig. 11(b).

The curve maintains its sinusoidal form when $T>0.1\times10^{-3}$ s as seen in Fig. 11(b). The introduction of the far-end crosstalk induces the massive broken structure depicted in Fig. 11(c). Additionally, the voltage curve exhibits a slight ascending and linear behaviour from -1800 V to -1750 V when 0 < T < 0.1 × 10^(-3) s. This behaviour changes from ascendant and linear to vertical and constant when T = 0.1 × 10^ (-3) s, as illustrated in Fig. 11(c). Moreover, the vertical and constant behaviour of the voltage increases from -1750 V to 0 V, as depicted in Fig. 11(c). Furthermore, the voltage behaviour changes again from vertical and constant to horizontal and constant when T > 0.1 × 10^(-3) s, as shown in Fig. 11(c). It appears that the far-end crosstalk is close to 0 V for a long period, as seen in Fig. 11(c), compared to what is seen in Figs. 7(c), 9(c) and 10(c). The period of action of the crosstalk phenomenon has significantly decreased.

Retrieval Number: 100.1/ijies.C78830912323
DOI: 10.35940/ijies.C7883.0910923
Journal Website: www.ijies.org

Published By:
Blue Eyes Intelligence Engineering and Sciences Publication (BEIESP)

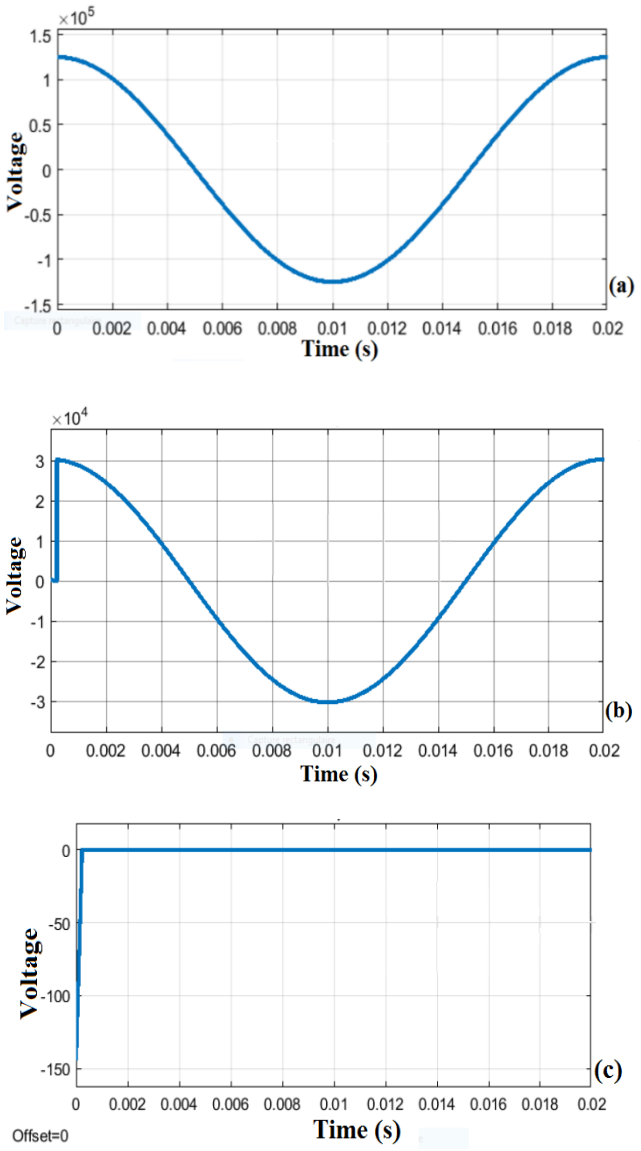

Figure 14 - Crosstalk Curves for z=444.196 ohms and φ=90°: (a) Source Voltage; (b) Near-End Crosstalk; (c) Far-End Crosstalk.

b. Crosstalk Phenomenon with Zc=444.196 ohms and φ=30°.

The impedance is maintained at Zc = 444.196 ohms, and the phase shift increases from φ = 15 ° to φ = 30 °. Then, we obtain Fig. (12). The source voltage is safeguarded as depicted in Figs. 11(a) and 12(a). The introduction of near-end crosstalk generates a significant fluctuation at the beginning of propagation. Besides, the time of apparition of this fluctuation is maintained to T=0.1×10^{-3} s as depicted in Fig. 12(b). Furthermore, the curve exhibits a microscopic linear and constant behaviour at 0.3 × 10^4 V when 0 < T < 0.1 × 10^(-3) s, as shown in Fig. 12(b). Thereafter, the voltage curve exhibits a long, vertical, and constant behaviour from 0.3 × 10^4 V to 1.80 × 10^4 V when T = 0.1 × 10^-3 s, as illustrated in Fig. 12(b). This fluctuation differs from that illustrated in Fig. 11(b). Moreover, the curve maintains its sinusoidal form when T > 0.1 × 10^ (- 3) s, as shown in Fig. 12(b).

The introduction of far-end crosstalk generates a large, broken structure, depicted in Fig. 12(c), similar to that illustrated in Fig. 11(c). After that, the voltage curve exhibits a minimal ascent and linear behaviour from -1750 V to -1700 V when 0 < T < 0.1 × 10^(-3) s. This behaviour changes from ascendant and linear to vertical and constant when T = 0.1 × 10^ (-3) s, as illustrated in Fig. 12(c). Additionally, the vertical and continuous behaviour of the voltage curve increases from -1700 V to 0 V, as shown in Fig. 12(c). Furthermore, the voltage behaviour is modified again from vertical and constant to horizontal and constant when T > 0.1 × 10^(-3) s, as seen in Fig. 12(c). It appears that the far-end crosstalk is close to 0 V for an extended period, as seen in Fig. 12(c). This behavior is similar to that illustrated in Fig. 11(c).

c. Crosstalk phenomenon with Zc=444.196 ohms and φ=60°.

The impedance is fixed at Zc = 444.196 ohms, and the phase shift increases from φ = 30 ° to φ = 60 °. Then, we obtain Fig. (13). The sinusoidal form of the source voltage is safeguarded as depicted in Fig. 13(a). The introduction of near-end crosstalk generates a significant fluctuation at the beginning of propagation. Besides, the time of apparition of this fluctuation is maintained to T=0.1×10^{-3} s as depicted in Fig. 13(b). Moreover, the curve exhibits a very small linear and constant behaviour at 0.1 × 10^4 V when 0 < T < 0.1 × 10^-3 s, as seen in Fig. 13(b). After, the voltage curve exhibits a long vertical
and constant behavior from 0.1×104V to 2.80×10^4 when T=0.1×10-3s as illustrated in Fig. 13(b). This fluctuation is longer compared to that seen in Fig. 12(b). Moreover, the curve maintains its sinusoidal form when T > 0.1 × 10^ (- 3) s, as shown in Fig. 12(b).

The introduction of far-end crosstalk generates a large broken structure, depicted in Fig. 13(c), similar to that illustrated in Fig. 12(c). Besides, the near-end crosstalk curve exhibits a microscopic ascending and linear behaviour from -1050V to -990V when 0<T<0.1×10^{-3} s. This behaviour is modified from ascendant and linear to vertical and constant when T = 0.1 × 10^ (-3) s, as shown in Fig. 13(c). Moreover, the vertical and continuous behaviour of the voltage curve increases from -990 V to 0 V, as shown in Fig. 13(c). Furthermore, the voltage behaviour is modified again from vertical and constant to horizontal and constant when T > 0.1 × 10^(-3) s, as seen in Fig. 13(c). It appears that the far-end crosstalk is close to 0 V for an extended period, as seen in Fig. 13(c). This behavior is similar to that illustrated in Fig. 12(c).

d. Crosstalk Phenomenon with Zc=444.196 ohms and φ=90°.

The impedance is fixed at Zc = 444.196 ohms, and the phase shift increases from φ = 60 ° to φ = 90 °. Hence, we obtain Fig. (14). The sinusoidal form of the source voltage is safeguarded as depicted in Fig. 14(a). The introduction of near-end crosstalk generates a significant fluctuation at the beginning of propagation. Besides, the time of apparition of this fluctuation is maintained to T=0.1×10^{-3} s as depicted in Fig. 14(b).

Moreover, the curve exhibits a very small linear and constant behaviour at 0 V when 0 < T < 0.1 × 10^(-3) s, as seen in Fig. 14(b). In addition, the voltage curve exhibits a long, vertical, and constant behaviour, varying from 0 V to 3.00 × 10^4 V when

Retrieval Number: 100.1/ijies.C78830912323
DOI: 10.35940/ijies.C7883.0910923
Journal Website: www.ijies.org

Published By:
Blue Eyes Intelligence Engineering and Sciences Publication (BEIESP)

T = 0.1 × 10^-3 s, as presented in Fig. 14(b). This fluctuation is longer compared to that seen in Fig. 13(b).
Furthermore, the curve maintains its sinusoidal form when T > 0.1 × 10^ (- 3) s, as shown in Fig. 14(b).

The introduction of far-end crosstalk generates a large broken structure, depicted in Fig. 14(c), similar to that illustrated in Fig. 13(c). Moreover, the near-end crosstalk curve exhibits a gradual ascending behaviour, varying from -140 V to 0 V when 0 < T < 0.1 × 10^ (- 3) s, as seen in Fig. 14(c). This behaviour is modified from a gradual ascent to a horizontal and constant behaviour when T > 0.1 × 10^(-3) s, as shown in Fig. 14(c). Furthermore, the horizontal and constant behaviours of the voltage curve are close to 0 V for an extended period, as shown in Fig. 14(c). Besides, this behaviour differs from that illustrated in Fig. 14(c). It appears that the far-end crosstalk significantly decreases as the phase shift increases.

E. Discussion

a. Crosstalk Values' Presentation

Some crosstalk voltage values coming from all the aforementioned figures are listed in Table 3.

Table 3- Results Obtained with Two Types of Lines

Z_C= 147.1874 ohms			
Near-End crosstalk	Far-End crosstalk	Phase shift (°)	Reduction rate
10 KV	0.50 KV	15	
9.5 KV	0.50 KV	30	
27 KV	0.32 KV	60	
10 KV	0.50 KV	90	
Zc=444.1967 ohms			
Near-End - crosstalk	Far-End - crosstalk	Phase shift (°)	Reduction rate
10 KV	-1.80 KV	15	**100%**
18 KV	-1.75 KV	30	
28 KV	-1.05 KV	60	
30 KV	-0.14 KV	90	

All the negative values of far-end crosstalk are directly related to 0V. Consequently, the reduction rate of crosstalk is considered to be 100% as seen in Table 3.

b. Analysis and Comparison of Results

Previous results in the literature				
Methods	Near-end crosstalk	Far-end crosstalk	Limits	Observations
Adapted terminations [21]	860mV	150mV	Increases the signal-to-crosstalk ratio	Zc1=147.2 Ω
Pseudo-adapted endings[21]	80mV	40mV	Does not eliminate	
	1000mV	200mV		Zc1=147.2 Ω
Our results for the contribution				
Pseudo-adapted endings	7.8588 kV	0V		Zc1=147.2 Ω zero crosstalk
	9.38kV	0V		Zc2=444.196Ω zero crosstalk

IV. CONCLUSION

We model the line through telegraphers' equations. Then, we use the Pseudomatched impedances method to reduce the crosstalk phenomenon in the line (victim driver). Some interesting results related to the values and physical impact of the crosstalk phenomenon during propagation are presented for two cases. Case 1 : Zc=147.1874 ohms and φ (15° ; 30° ; 60° ; 90°). (i) The source voltage exhibits a sinusoidal form. (ii) The near-end crosstalk generates a small broken point (small fluctuation) at the beginning of the propagation. As the phase shift increases, we note the following points. This small fluctuation is changed to a huge fluctuation. The source voltage form is modified from sinusoidal to linear. Thereafter, this sinusoidal form is also transformed from linear to sinusoidal, associated with a big broken point. Similar behaviour is obtained for different values of the phase shift (φ = 15° and φ = 90°). (iii) The far-end crosstalk induces a huge broken point (huge broken fluctuation). Then, the sinusoidal form of the source voltage is transformed into a huge broken fluctuation. The general aspect of this significant fluctuation remains intact as the phase shift increases. (iv) The crosstalk phenomenon decreases the voltage values during propagation. The far-end crosstalk presents the lower voltage values compared to the near-end crosstalk. (v) The cancellation time of the crosstalk phenomenon is T=0.6 ms. Case 2 : Zc=444.196 ohms and φ (15° ; 30° ; 60° ; 90°). (i) The near-end crosstalk generates a small broken point (small fluctuation) which increases as the phase shift increases. The voltage curve exhibits fluctuations associated with a sinusoidal form. (ii) The far-end crosstalk induces an opposite huge broken fluctuation compared to that obtained in the first case. (iii) The cancellation time of the crosstalk phenomenon is decreased from T=0.6 ms to T=0.1 ms.

ACKNOWLEDGMENTS

The authors thank the anonymous reviewers and the associate Editor in charge of this manuscript. Special thanks to the conference of Directors of Blue Eyes Intelligence Engineering and Sciences Publication (BEIESP), which has decided to publish this manuscript without any author publication charges (APC). We also want to thank Professor Salome Ndjakomo Essiane, Chairman of ACRITEE (Cameroonian Association for Research and Innovation in Environmental and Energy Technologies), for the specific contribution of his scientific group.

DECLARATION STATEMENT

Funding/ Grants/ Financial Support	No, I did not receive.
Conflicts of Interest/ Competing Interests	No conflicts of interest to the best of our knowledge.
Ethical Approval and Consent to Participate	No, the article does not require ethical approval or consent to participate, as it presents evidence that is not subject to interpretation.
Availability of Data and Material/ Data Access Statement	Not relevant.
Authors Contributions	All authors have equal participation in this article.

REFERENCES

1. Chunming Qiao, Member, ZEEE, Rami Georges Melhem, Donald M. Chiarulli, and Steven P. Levitan, 'A Time Domain Approach for Avoiding Crosstalk in Optical Blocking Multistage Interconnection Networks. JOURNAL OF LIGHTWAVE TECHNOLOGY, VOL 12, 10 OCTOBER 1994. https://doi.org/10.1109/50.337500
2. Yunfeng Shen, Kejie Lu, and Wanyi Gu, Coherent and Incoherent Crosstalk Coherent and Incoherent Crosstalk in WDM Optical Networks. JOURNAL OF LIGHTWAVE TECHNOLOGY, VOL. 17, NO. 5, MAY 1999 https://doi.org/10.1109/50.762889
3. Faten Sahel, Pascal Guilbault, Farouk Vallette, Sylvain Feruglio. A Crosstalk Modelling Method between a Power Supply and a Nearby Signal in High-density Interconnection PCBs. 2021 22nd International Symposium on Quality Electronic Design (ISQED), Apr 2021, Santa Clara, CA, United States. pp.227-232, ff10.1109/ISQED51717.2021.9424304ff. ffhal-03225181ff . https://doi.org/10.1109/ISQED51717.2021.9424304
4. Rza Bashirov *, Tolgay Karanfiller, On path-dependent loss and switch crosstalk reduction in optical networks. Information Sciences 180 (2010) 1040–1050. https://doi.org/10.1016/j.ins.2009.11.017
5. Isaak E. Müller, Jacob R. Rubens, Tomi Jun, Daniel Graham, Ramnik Xavier and Timothy K. Lu, Gene networks that compensate for crosstalk with crosstalk. NATURE COMMUNICATIONS (2019) 10:4028 | https://doi.org/10.1038/s41467-019-12021-y https://doi.org/10.1038/s41467-019-12021-y
6. E. L. Goldstein, L. Eskildsen, and A. F. Elrefaie, "Performance implications of component crosstalk in transparent lightwave networks," IEEE Photon. Technol. Lett., vol. 6, pp. 657–660, May 1994. https://doi.org/10.1109/68.285571
7. C. S. Li and F. Tong, "Crosstalk and interference penalty in all-optical networks using static wavelength routers," J. Lightwave Technol., vol. 14, pp. 1120–1126, June 1996. https://doi.org/10.1109/50.511613
8. H. Takahashi, K. Oda, and H. Toba, "Impact of crosstalk in an arrayed-waveguide multiplexer on N N optical interconnection," J. Lightwave Technol., vol. 14, pp. 1097–1105, June 1996. https://doi.org/10.1109/50.511611
9. M.M. Vaez, C.T. Lea, Strictly nonblocking directional-coupler based switching networks under crosstalk constraint, IEEE Transactions on Communication 48 (2000) 316–323. https://doi.org/10.1109/26.823564
10. A.K. Katangur, S. Akkaladevi, Y. Pan, Analyzing the performance of optical multistage interconnection networks with limited crosstalk, Cluster Computing 10 (2007) 241–250 https://doi.org/10.1007/s10586-007-0018-7
11. X. Jiang, H. Sheng, M.R. Khandker, S. Horiguchi, Blocking behaviors of crosstalk-free optical banyan networks on vertical stacking, IEEE/ACM Transactions on Networking 11 (2003) 982–993. https://doi.org/10.1109/TNET.2003.820425
12. Rowland, M. A. & Deeds, E. J. Crosstalk and the evolution of specificity in two-component signalling. Proc. Natl Acad. Sci. USA 111, 5550–5555 (2014). https://doi.org/10.1073/pnas.1317178111
13. S. D. Dods, J. P. R. Lacey, and R. S. Tucker, "Homodyne crosstalk in WDM ring and bus networks," IEEE Photon. Technol. Lett., vol. 9, pp. 1285–1287, Sept. 1997. https://doi.org/10.1109/68.618506
14. Rhodius, V. A. et al. Design of orthogonal genetic switches based on a crosstalk map of σs, anti-σs, and promoters. Mol. Syst. Biol. 9, 702 (2013). https://doi.org/10.1038/msb.2013.58
15. Capra, E. J., Perchuk, B. S., Skerker, J. M. & Laub, M. T. Adaptive mutations that prevent crosstalk enable the expansion of paralogous signalling protein families. Cell 150, 222–232 (2012) https://doi.org/10.1016/j.cell.2012.05.033
16. Guo, X. & Wang, X. F. Signaling cross-talk between TGF-β/BMP and other pathways. Cell. Res. 19, 71–88 (2009). https://doi.org/10.1038/cr.2008.302
17. Vert, G. & Chory, J. Crosstalk in cellular signalling: background noise or the real thing? Dev. Cell 21, 985–991 (2011) https://doi.org/10.1016/j.devcel.2011.11.006
18. Wu, F., Menn, D. J. & Wang, X. Quorum-sensing crosstalk-driven synthetic circuits : from unimodality to trimodality. Chem. Biol. 21, 1629–1638 (2014). https://doi.org/10.1016/j.chembiol.2014.10.008
19. Morey, K. J. et al. Crosstalk between endogenous and synthetic components - synthetic signalling interacts with endogenous components. Biotechnol. J. 7, 846–855 (2012). https://doi.org/10.1002/biot.201100487
20. T. Ditchi. "les lignes de transmission". Course on transmission lines. University of SORBONNE, page 1-74, (2015).
21. S. Roblot. "Caractérisation des couplages électromagnétiques dans les réseaux filaires cuivre en vue d'optimiser les transmissions à haut débit". Doctorate thesis of the University of Limoges. 1-164, (2007).
22. M. Kachout, "Interference reduction for RF signal integrity". 1-118, (2016).
23. F. Broydé, "Radically eliminating crosstalk in interconnections" Electronique, No.140, pp. 57-61, 2003.

AUTHOR PROFILE

Dr. Jacquie Therese NGO BISSE, Laboratory of Electrotechnics, Automatics and Energy, Department of Maintenance, Higher Technical Teachers Training College (HTTTC) of EBOLOWA, University of EBOLOWA, P.O. Box 886, Ebolowa, Cameroon. Jacquie Therese Ngo Bisse is a specialist in Electronic Systems and maintenance. She is a Ph.D. holder from the University of Douala. She is currently an Associate Lecturer at the Higher Technical Teacher's Training College of Ebolowa, affiliated with the University of Ebolowa in Cameroon. His research is linked to Electronic systems and Power Systems modelling.

Dr. Bedel Giscard ONANA ESSAMA, Laboratory of Electrotechnics, Automatics and Energy, Department of Electrical Engineering, Higher Technical Teachers Training College (HTTTC) of EBOLOWA, University of EBOLOWA, P.O. Box 886, Ebolowa, Cameroon. Bedel Giscard Onana Essama is a specialist in Energy-Electric and Electronic Systems. He is a Ph.D. holder from the University of Yaounde 1. He is currently an Associate Lecturer at the Higher Technical Teacher's Training College of Ebolowa, affiliated with the University of Ebolowa in Cameroon. His research is linked to Energetic systems, Power Systems Modelling, complex systems modelling, Nonlinear Dynamics, optical fibre, and Medical Physics.

Dr. Joseph KOKO KOKO, Laboratory of Electrotechnics, Automatics and Energy, Department of Electrical Engineering, Higher Technical Teachers Training College (HTTTC) of EBOLOWA, University of EBOLOWA, P.O. Box 886, Ebolowa, Cameroon. Joseph KOKO KOKO is a specialist in Energic systems and power lines. He is a Ph.D. holder from the University of Douala. He is currently working with the Higher Technical Teacher's Training College of Ebolowa, associated with the University of Ebolowa in Cameroon. His research is linked to Power Systems and Power Electronics.

Professor Jacques ATANGANA, Laboratory of Electronics, Electrotechnics and Automatics, Department of Physics, Higher Teachers Training College (HTTC) of Yaoundé, University of Yaoundé 1, P.O. Box 47, Yaoundé, Cameroon. Jacques Atangan is a specialist in electronic systems. He is a Ph.D. holder from the University of Yaoundé 1. He is currently a professor at the Higher Teacher's Training College of Yaoundé, affiliated with the University of Yaoundé 1 in Cameroon. His research is related to Electrical transmission lines and the modelling of complex systems.

Professor Salome NDJAKOMO ESSIANE, Laboratory of Electrotechnics, Automatics and Energy, Department of Electrical Engineering, Higher Technical Teachers Training College (HTTTC) of EBOLOWA, University of EBOLOWA, P.O. Box 886, Ebolowa, Cameroon. Salomé Ndjakomo Essiane is a specialist in electronics and optoelectronics. She is a Ph.D. holder from Ibn Zohr University in Morocco. She is currently a professor at the Higher Technical Teacher's Training College of Ebolowa, affiliated with the University of Ebolowa in Cameroon. Her research is related to Electrical power engineering and power systems modelling.

APPENDIX

A.1.

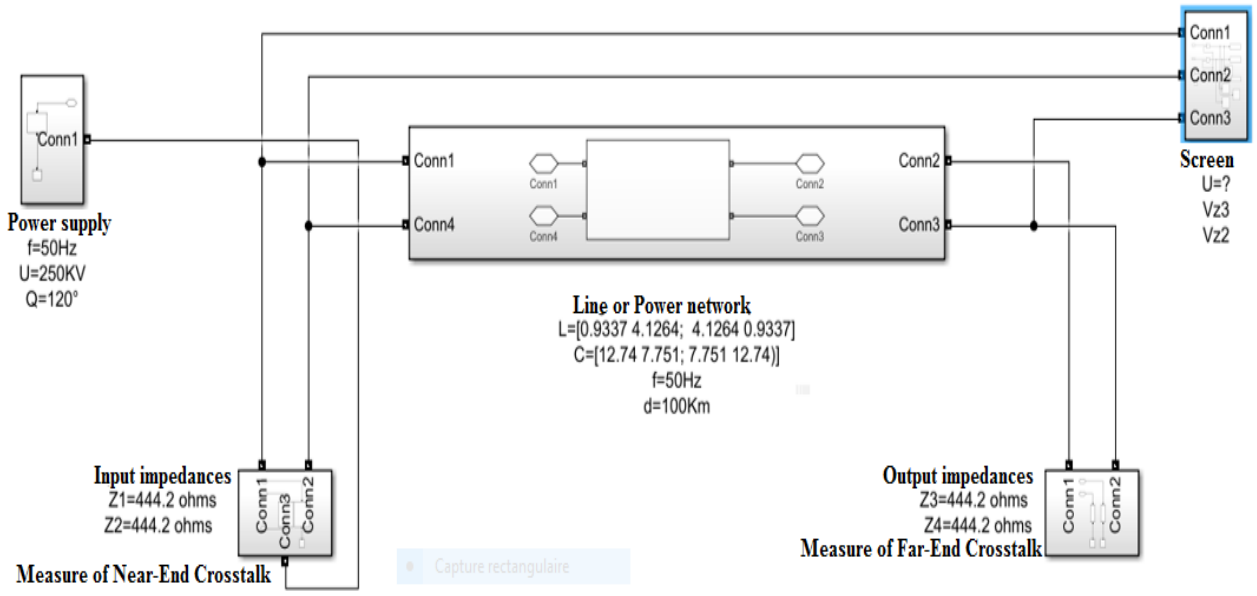

Fig. 4. Simulink Diagram of the Power Network

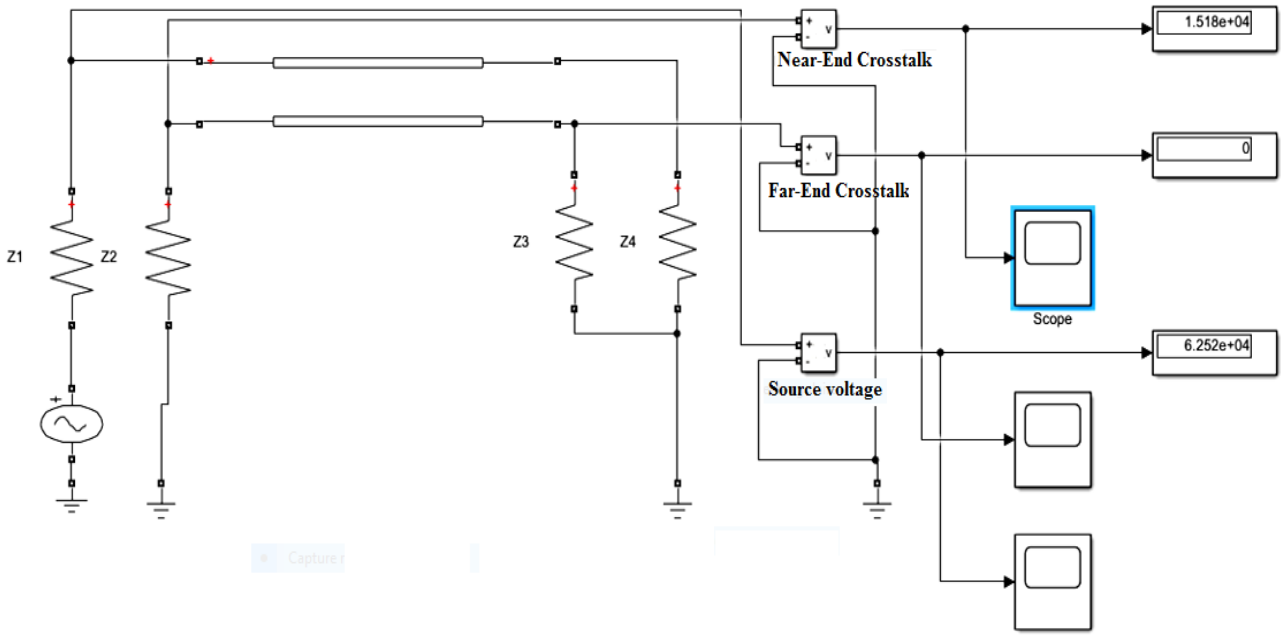

Fig. 6. Internal Parameters of the Power Network